A methodology to compute mixing ratios with uncertain end-members

J. Carrera, E. Vázquez-Suñé, O. Castillo, and X. Sánchez-Vila

Department Geotechnical Engineering and Geosciences, School of Civil Engineering, Technical University of Catalonia, Barcelona, Spain

[1] Mixing calculations involve computing the ratios in which two or more end-members are mixed in a sample. Mixing calculations are useful for a number of tasks in hydrology, such as hydrograph separation, water or solute mass balances, and identification of groundwater recharge sources. Most methods available for computing mixing ratios are based on assuming that end-member concentrations are perfectly known, which is rarely the case. Often, end-members cannot be sampled, and their concentrations vary in time and space. Still, much information about them is contained in the mixtures. To take advantage of this information, we present here a maximum likelihood method to estimate mixing ratios, while acknowledging uncertainty in end-member concentrations. Maximizing the likelihood of concentration measurements with respect to both mixing ratios and end-member concentrations leads to a general constrained optimization problem. An algorithm for solving this problem is presented and applied to two synthetic examples of water mixing problems. Results allow us to conclude that the method outperforms traditional approaches, such as least squares or linear mixing, in the computation of mixing ratios. The method also yields improved estimates of end-member concentrations, thus enlarging the potential of mixing calculations. The method requires defining the reliability of measurements, but results are quite robust with respect to the assumed standard deviations. A nice feature of the method is that it allows for improving the quality of computations by increasing the number of samples and/or analyzed species.   *INDEX TERMS:* 1831 Hydrology: Groundwater quality; 1829 Hydrology: Groundwater hydrology; 1836 Hydrology: Hydrologic budget (1655); *KEYWORDS:* end-member, groundwater, mixing, salt balance, tracer, water balance

Citation: Carrera, J., E. Vázquez-Suñé, O. Castillo, and X. Sánchez-Vila (2004), A methodology to compute mixing ratios with uncertain end-members, *Water Resour. Res.*, *40*, W12101, doi:10.1029/2003WR002263.

1. Introduction

[2] Mass balance of chemical species is often used in hydrology and related sciences to aid in the evaluation of water balances. Its simplest form consists of measuring the concentrations of any conservative species in inflowing and outflowing waters and, assuming continuity, establishing the mass balance of solute and water as (see Figure 1):

$$Q_1 x_1 + Q_2 x_2 = Q_p y_p \qquad (1)$$

$$Q_1 + Q_2 = Q_p, \qquad (2)$$

where Q_1 and Q_2 are the inflow rates, x_1 and x_2 are the corresponding concentrations (in this example only two end-members are considered) and Q_p and y_p are the outflow rate and concentration, respectively. Actually, flow rates can be eliminated from these equations. Dividing (1) and (2) by Q_p leads to

$$\delta_{p1} x_1 + \delta_{p2} x_2 = y_p \qquad (3)$$

$$\delta_{p1} + \delta_{p2} = 1, \qquad (4)$$

where δ_{p1} and δ_{p2} are the mixing ratios of end-members 1 and 2 in sample p. If x_1 is not equal to x_2, then equations (3) and (4) can be easily solved for δ_{p1} and δ_{p2}. In turn, measurement of any one of the flow rates allows deriving the others as $Q_1 = \delta_{p1} Q_p$ and $Q_2 = \delta_{p2} Q_p$. In short, mixing ratios help in deriving the mass balance of a water body.

[3] These calculations are basic enough to be described in classical hydrogeology textbooks [e.g., *Custodio and Llamas*, 1984; *Zuber*, 1986]. We have included them here to introduce the basic notation. However, we wish to stress that they are used in all branches of hydrology. Recent applications include the evaluation of groundwater inflows to surface water bodies [*Ojiambo et al.*, 2001] or vice versa [*Plummer et al.*, 1998; *Stute et al.*, 1997]. They have also been used for the purpose of hydrograph separation [*Joerin et al.*, 2002] and to evaluate the sources of recharge to groundwater [*Pitkänen et al.*, 1999]. The original motivation of our work was the identification and quantification of recharge sources in the city of Barcelona, where up to eight end-members had been identified [*Vázquez-Suñé et al.*, 1997]. However, other urban areas face similar problems of quantifying a large number of end-members [*Yang et al.*, 1999; *Suk and Lee*, 1999].

[4] Mixing calculations are also used in other branches of earth sciences. For example, erosion rates can be determined from the composition of suspended and dissolved solids in
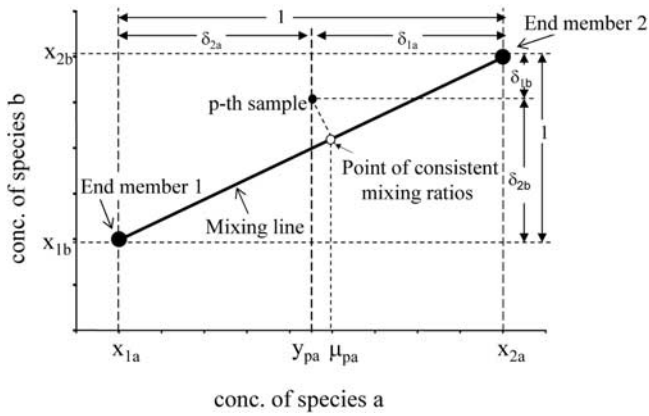
Figure 1. Illustration of mixing calculations. Given the concentrations (x_{1a} and x_{2a}) of a chemical species, a, in two source waters (end-members), it is possible to derive the mixing ratios in mixed sample, p, from its concentration y_{pa} (δ_{1a} and δ_{2a}, respectively, shown above). When the concentrations of two (a and b) or more species are available, measurement errors may lead to inconsistent mixing ratios. In the example of the figure, mixing ratios derived from species a are nearly identical for the two end-member ($\delta_{1a} \sim \delta_{2a}$). However, if species b is used, one would conclude that the proportion of end-member 2 (δ_{2b}) is much larger than that of end-member 1 (δ_{1a}). Consistent mixing ratios can be obtained by least squares, which implies projecting the data point onto the mixing line.

rivers [*Allègre et al.*, 1996; *Roy et al.*, 1999]. Emission inventories into the atmosphere can also be obtained with the aid of mixing calculations [*Biesenthal and Shepson*, 1997]. These are also used to discriminate between mineral dissolution and atmospheric deposition as the origin of solutes in mountain rivers [*Johnson et al.*, 2001; *Williams et al.*, 2001].

[5] Mixing analyses are essentially done with conservative tracers. However, they can also be used to identify reaction processes. In this case, departures from mixing lines (or planes) are attributed to chemical reactions [*Skov et al.*, 1997; *Pitkänen et al.*, 1999].

[6] Practical application of mixing ratios calculations may require introducing some complexity in equations (1) and (2). For example, if more than one species is available, mixing ratios derived from each species may not be consistent. A least squares approach may then be used to minimize what are often termed analytical errors. Actually, when concentration measurements from two species are known, one can derive the mixing ratios for three end-members, as illustrated in Figure 2. The methodology can be easily extended to any number of sources, n_e, provided that concentrations of, at least, $n_e - 1$ conservative species are available.

[7] An alternative mixing model to the one discussed so far is the mixing cells model [*Campana and Simpson*, 1984], which consists of cells or reactors that exchange water and solutes. This model has been generalized by Adar and coworkers. They use a suite of chemical and isotopic tracers to identify spatially varying recharge [*Adar and Nativ*, 2000; *Adar et al.*, 1988, 1992].

[8] In summary mixing models are widely used in all branches of hydrology and also in other sciences. While it is widely recognized that there is always some uncertainty involved in the evaluation of the end-members concentrations, they are assumed to be accurately known in most practical applications.

[9] Uncertainty in end-member flows and concentrations derive not primarily from analytical error but from spatial and temporal variability in the end-member flows and compositions as well as errors in the conceptual model of the flow system. For example, in the case of rainfall, one does not know when recharge does occur. As a result, it is difficult to characterize the portion of precipitation actually entering into soil and aquifer, even if the spatial and temporal variability of rainfall were exhaustively sampled. This is one of the main handicaps for the use of H and O isotopes. A similar problem occurs with river inflows into aquifers, which may concentrate during floods. Reversely, flux averaged concentrations should be used when characterizing aquifer discharges to perform salt balances in rivers and lakes. However, conventional sampling yields resident concentrations. This, together with recharge variability makes the resulting mixing ratios highly uncertain [*Joerin et al.*, 2002].

[10] In short, accurate definition of the concentrations in the inflows to any body of water is very difficult. On the other hand, concentrations of mixed samples are likely to be less uncertain that those of end-members. The reason is that uncertainties in mixed samples are due mainly to analytical errors, as dilution mechanisms in the aquifer filter most temporal fluctuations in end-members. This smaller uncertainty suggests that it may be possible to use actual concentration data to impose constraints on valid end-members concentrations, as illustrated in Figure 3.

[11] The objective of our work is to derive a methodology to identify mixing ratios in the case of uncertain end-members using the concentrations of mixed samples to reduce such uncertainty. The proposed approach is an extension of that by *Kent et al.* [1990], who derived a methodology for fitting planes to uncertain data. Our extension is twofold [*Castillo*, 2000]. First, we generalize
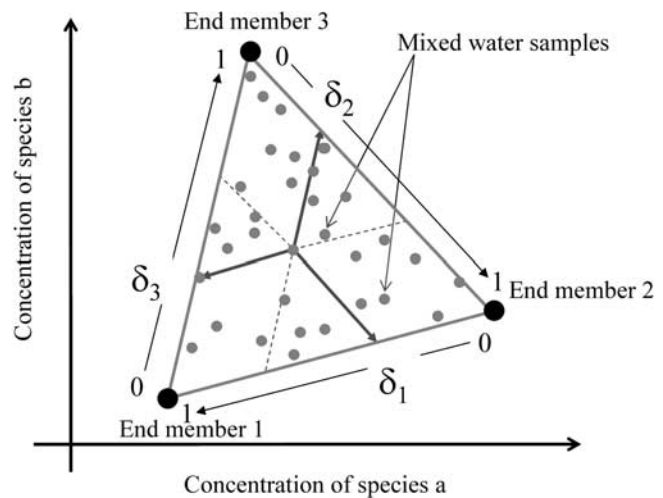

Figure 2. Definition of mixing ratios in a problem with three end-members and two species.
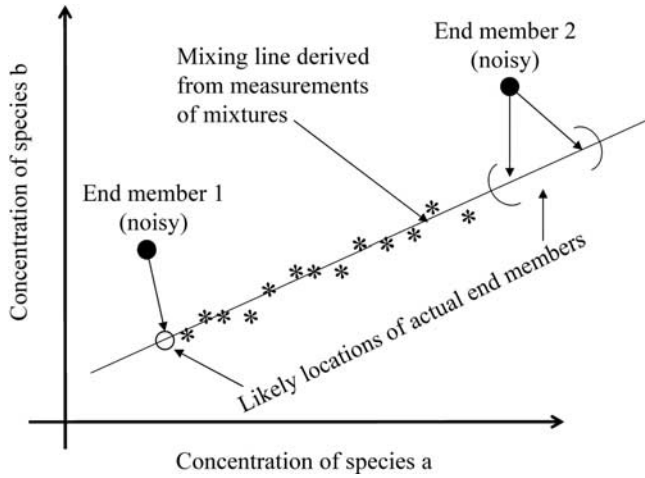
Figure 3. Mixed water samples often define mixing lines more accurately than "noisy" end-member concentrations. In such a case, taking mixing constraints into account may significantly reduce uncertainty in end-member concentrations by imposing consistency. Consistency is meant in two ways. First, end-members should fall in the mixing line. Second, mixed waters should fall within the interval defined by end-members. This second condition does not constrain the concentration of end-member 2 but reduces the uncertainty of end-member 1.

it to the case of an arbitrary number of unknowns (the previous authors only estimated the two coefficients of the plane equation). Second, we apply it to mixing equations. This second extension presupposes that all mixing ratios add up to 1 and be positive.

2. Methodology

2.1. Problem Statement and Solution Steps

[12] The problem is to find the proportions in which ne end-member waters are mixed in np samples. To this end, the concentrations of ns species are measured in each of the mixtures. Measurements are also available for the concentrations of end-members. That is, a total of $nw = ne + np$ full analyses are available. Measurement uncertainty is quantified through covariance matrices.

[13] The proposed algorithm consists of the following steps: (0) Initialization, consisting of the definition of initial mixing ratios by conventional least squares, assuming that the concentrations of end-members are known; (1) given the mixing ratios, maximize the likelihood function to estimate the expected values of mixture and end-member concentrations; (2) given the expected values of mixture and end-member concentrations, maximize the likelihood to obtain the mixing ratios; (3) repeat steps 1 and 2 until convergence. Following is a description of each of these steps and a derivation of the necessary equations.

2.2. Conventional Least Squares for Each Sample Assuming Known End-Members

[14] The mixing equation of each mixture p can be written as a generalization of (4):

$$y_{ps} = \sum_{e=1}^{ne} \delta_{pe} x_{es} + \varepsilon_{ps} \qquad s = 1, .., ns, \qquad (5)$$

where y_{ps} and x_{es} are the concentrations of species s in sample p and end-member e, respectively, δ_{pe} is the proportion of end-member e in mixture p, and ε_{ps} is an error. The latter is often termed measurement error, even though it may be caused not only by measurements, but also by conceptual errors (e.g., nonconstant end-member concentration). Following previous work [*Carrera and Neuman*, 1986; *Medina and Carrera*, 1995] we formulate the estimation problem in a maximum likelihood framework. Assuming that the concentrations of end-members are known and that errors are normally distributed (the effect of this assumption can be relaxed by forcing the variance to depend on concentration, i.e., constant close to the detection limit and increasing the standard deviation for lower concentrations), the likelihood function is

$$L_p = \exp\left[-\frac{1}{2}\left(\mathbf{y}_p - \mathbf{F}\delta_p\right)^t \mathbf{A}_p^{-1}\left(\mathbf{y}_p - \mathbf{F}\delta_p\right)\right], \qquad (6)$$

where $\mathbf{y}_p$ is the vector of all species measured in the pth sample $[\mathbf{y}_p^t = (y_{p1}, \cdots, y_{ps}, \cdots y_{pns})]$, $\mathbf{A}_p$ is their covariance matrix, $\mathbf{F}$ is the $ns \times ne$ dimensional matrix of all chemical analyses of end-members $[\mathbf{F} = \{x_{es}\}]$ and δ_p is the vector of mixing ratios $[\delta_p^t = (\delta_{p1}, \cdots \delta_{pe}, \cdots, \delta_{p\,ne})]$. This latter vector must satisfy the constraint that mixing ratios add up to 1:

$$\delta_p^t \mathbf{1}_{ne} = 1, \qquad (7)$$

where $\mathbf{1}_{ne}$ is a ne-dimensional vector of 1's.

[15] In order to maximize (6) subject to (7), we build the Lagrangian function

$$\mathcal{L}_p = -\ln L_p + \lambda_p \delta_p^t \mathbf{1}_{ne}, \qquad (8)$$

where λ_p is a Lagrange multiplier.

[16] Taking derivatives of (8) with respect to δ_p and λ_p leads to the well know linearly constrained least squares equations:

$$\begin{pmatrix} \mathbf{F}^t \mathbf{A}_p \mathbf{F} & \mathbf{1}_{ne} \\ \mathbf{1}_{ne}^t & 0 \end{pmatrix} \begin{pmatrix} \delta_p \\ \lambda_p \end{pmatrix} = \begin{pmatrix} \mathbf{F}_p^t \mathbf{A}_p^{-1} \mathbf{y}_p \\ 1 \end{pmatrix}. \qquad (9)$$

It should be noticed that, if the same species are analyzed for all samples and they have the same covariance matrix, then the coefficient matrix in (9) will also be the same for all samples. This, together with the fact that the dimension of the system $(ne + 1)$ is relatively small, makes it very easy to obtain the mixing ratios for each sample separately. The only difficulty arises from the fact that mixing ratios must also satisfy the constraint

$$0 \leq \delta_{pe} \leq 1. \qquad (10)$$

This, together with (7) defines the set of feasible solutions, which is a simplex set. Its vertices are obtained by setting each mixing ratio to one while letting the others be equal to zero. In general, this type of problems can be difficult (see, e.g., *Gill* [1981] for a discussion). In our case, however, constraint (7) implies that it is sufficient to impose nonnegativity (the condition $\delta_{pe} \leq 1$ is satisfied automatically). In fact, since $\mathbf{A}_p$ is positive definite, the

objective function is convex. As a result, it is sufficient to set to zero mixing ratios that are negative after the initial solution of (9), and solve again (9) for the remaining ratios.

2.3. Formulation of the Problem for Known Mixing Ratios, the Likelihood Function

[17] As stated, the objective is to find the most likely concentrations of samples and end-members that jointly satisfy the mixing equations, provided that mixing ratios are known. To this end, we define the vector of all concentration data, $\mathbf{z}$, which consists of ns vectors $\mathbf{z}_s$ containing the analyses of each species s at all end-members and samples:

$$\mathbf{z}_s^t = \left(\mathbf{x}_s^t, \mathbf{y}_s^t\right) = [x_{s1}, \ldots, x_{s\,ne}, y_{s1}, \ldots, y_{s\,np}] \qquad s = 1, \ldots, ns. \tag{11}$$

Let $\mathbf{\mu}_s$ and $\mathbf{\mu}$ be the expected values of $\mathbf{z}_s$ and $\mathbf{z}$, respectively. Because we are working with all samples together, mixing ratios are best written as a matrix, rather than as a vector:

$$\mathbf{\Delta} = \begin{bmatrix} \mathbf{\delta}_1^t \\ \mathbf{\delta}_p^t \\ . \\ . \\ \mathbf{\delta}_{np}^t \end{bmatrix} = \begin{bmatrix} \delta_{11} & \delta_{1e} & . & . & \delta_{1\,ne} \\ \delta_{p1} & \delta_{pe} & . & . & \delta_{p\,ne} \\ . & . & . & . & . \\ . & . & . & . & . \\ \delta_{np1} & \delta_{npe} & . & . & \delta_{np\,ne} \end{bmatrix}. \tag{12}$$

For conciseness, it is convenient to define $\mathbf{\Gamma} = (\mathbf{\Delta}, -\mathbf{I}_{np \times np})$, the extended mixing ratios matrix. This is used to define the constraints on mixing ratios, by writing (7) simultaneously for all species as

$$\mathbf{\Gamma}\, \mathbf{1}_{ne+np} = \mathbf{0}_{np}. \tag{13}$$

Similarly, constraints on the means are obtained by writing the mixing equations in matrix form assuming the errors are zero mean:

$$\mathbf{\Gamma}\, \mathbf{\mu}_s = \mathbf{0}_{np} \qquad s = 1, \ldots, ns, \tag{14}$$

which expresses the expected value of (5) for all samples. The normality assumption allows us to write the likelihood function as

$$L = \exp\left[-\frac{1}{2}(\mathbf{z}-\mathbf{\mu})^t \mathbf{A}^{-1}(\mathbf{z}-\mathbf{\mu})\right], \tag{15}$$

where $\mathbf{A}$ is the covariance matrix of all chemical analyses taken as known. In our implementation we have assumed, for simplicity, but without loss of generality, that errors in one species are independent of errors in other species. However, for any species, they may well be correlated across samples. This implies that we will be able to filter out systematic errors caused by improper handling of one species. This assumption simplifies significantly the speci-

fication of $\mathbf{A}$. Also, it simplifies computations, because it allows us to rewrite (15) as

$$f = \ln L = \sum_{s=1}^{ns} \left[-\frac{1}{2}(\mathbf{z}_s - \mathbf{\mu}_s)^t \mathbf{A}_s^{-1}(\mathbf{z}_s - \mathbf{\mu}_s)\right]. \tag{16}$$

This function has to be maximized with respect to $\mathbf{\Delta}$ and $\mathbf{\mu}$, while ensuring that constraints (13) over $\mathbf{\Delta}$ and (14) over $\mathbf{\mu}$ are satisfied. We propose to do it in two stages: first, obtain $\mathbf{\mu}$ given $\mathbf{\Delta}$ and, second, obtain $\mathbf{\Delta}$ given $\mathbf{\mu}$. These steps are repeated until convergence.

2.4. Estimation of $\mathbf{\mu}$, Assuming $\mathbf{\Delta}$ Fully Known

[18] Maximization of (16) can be done separately for each species (if we had assumed that errors were correlated across species, the equations would have been larger, but the formalist remains identical). In order to impose constraint (14), we first build the Lagrangian:

$$L = -\frac{1}{2}(\mathbf{z}_s - \mathbf{\mu}_s)^t \mathbf{A}_s^{-1}(\mathbf{z}_s - \mathbf{\mu}_s) + \mathbf{\lambda}_s^t\, \mathbf{\Gamma}\mathbf{\mu}_s, \tag{17}$$

where $\mathbf{\lambda}_s$ is the $np -$ dimension vector of Lagrange multipliers. Taking derivatives of $\mathscr{L}$ with respect to $\mathbf{\mu}_s$ and $\mathbf{\lambda}_s$ and setting them to zero leads to

$$\mathbf{\mu}_s = \mathbf{z}_s + \mathbf{A}_s\, \mathbf{\Gamma}^t\mathbf{\lambda}_s, \tag{18}$$

where $\mathbf{\lambda}_s$ is obtained by multiplying this equation by $\mathbf{\Gamma}$ while bearing (14) in mind. This yields

$$\mathbf{\lambda}_s = -\mathbf{C}_s\mathbf{\Gamma}\mathbf{z}_s, \tag{19}$$

where $\mathbf{C}_s = (\mathbf{\Gamma}\mathbf{A}_s\mathbf{\Gamma}^t)^{-1}$. Finally, substituting this vector back in (18) yields the solution we were seeking:

$$\mathbf{\mu}_s = \mathbf{z}_s - \mathbf{A}_s\mathbf{\Gamma}^t(\mathbf{\Gamma}\mathbf{A}_s\mathbf{\Gamma}^t)^{-1}\mathbf{\Gamma}\mathbf{z}_s. \tag{20}$$

It is interesting to notice from (20) that $\mathbf{\mu}_s$ is simply the projection of data $\mathbf{z}_s$ on the mixing equations (5). The effect of projecting measurements of end-member concentrations into the mixing equation was illustrated in Figure 3. Similarly, the projection of mixtures data onto the mixing line was illustrated in Figure 1. The only peculiarity of (20) is that it was derived assuming that the mixing ratios were known. Their evaluation is updated in the next step.

2.5. Derivation of the Equations for $\mathbf{\Delta}$, Assuming Known $\mathbf{\mu}$

[19] The objective now is to find the mixing ratios ($\mathbf{\Delta}$) that maximize the likelihood, knowing that the expected values of concentrations are given by (20). Substituting (20) in (16) and applying (14) yields the updated objective function. In order to maximize it with respect to $\mathbf{\Delta}$ while imposing constraints (13), we build again a Lagrangian function:

$$\mathscr{L} = -\frac{1}{2}\sum_{s=1}^{ns} \mathbf{z}_s^t\mathbf{\Gamma}^t(\mathbf{\Gamma}\mathbf{A}_i\mathbf{\Gamma}^t)^{-1}\mathbf{\Gamma}\mathbf{z}_s + \mathbf{\beta}^t\mathbf{\Gamma}\, \mathbf{1}, \tag{21}$$

where $\mathbf{\beta}$ is the np dimensional vector of Lagrange multipliers. In order to maximize this Lagrangian, it is necessary

to take derivatives of (21) with respect to $\boldsymbol{\Delta}$ and $\boldsymbol{\beta}$. This is somewhat complex, but facilitated by taking into account that

$$\frac{\partial}{\partial \boldsymbol{\Delta}} \left(\mathbf{a}^t \boldsymbol{\Gamma} \, \mathbf{b} \right) = \mathbf{a} \mathbf{b}_{ne}^t, \qquad (22)$$

where $\mathbf{a}$ and $\mathbf{b}$ are arbitrary constant vectors of dimensions np and nw, respectively, and $\mathbf{b}_{\mathrm{ne}}$ is a ne-dimensional vector equal to the first ne components of $\mathbf{b}$. Equation (22) is easily derived by considering that $\partial \Gamma_{ij}/\partial \delta_{kl}$ equals 1 if $i = k$ and $j = l$, and 0 otherwise.

[20] Taking derivatives of (21) with respect to $\boldsymbol{\Delta}$ and $\boldsymbol{\beta}$ while bearing (22) in mind and making use of (19) and (20) leads to

$$\partial \mathscr{L}/\partial \boldsymbol{\Delta} = \mathbf{F} = \sum_{s=1}^{ns} \lambda_s \boldsymbol{\mu}_{sne}^t + \boldsymbol{\beta} \mathbf{1}_{ne}^t = \mathbf{0} \qquad (23a)$$

$$\partial \mathscr{L}/\partial \boldsymbol{\beta} = \mathbf{f} = \boldsymbol{\Gamma} \mathbf{1}_{nw} = \mathbf{0}. \qquad (23b)$$

This is a nonlinear system with $np \times ne + np$ equations and unknowns ($np \times ne$ mixing ratios, $\boldsymbol{\Delta}$, and np Lagrange multipliers, $\boldsymbol{\beta}$). We have solved it using the Newton-Raphson method, while imposing the nonnegativity constraints discussed in section 2.2. The solution method is outlined in the following section.

2.6. Newton-Raphson Solution of the Minimum Conditions

[21] For solving the nonlinear system (23), we have expanded $\mathbf{F}$ with respect to $\boldsymbol{\Delta}$:

$$\mathbf{F}^{k+1} \approx \mathbf{F}^k + \frac{\partial \mathbf{F}}{\partial \boldsymbol{\Delta}} \left(\boldsymbol{\Delta}^{k+1} - \boldsymbol{\Delta}^k \right). \qquad (24)$$

Using (24), (23) is approximated as

$$\begin{pmatrix} \dfrac{\partial \mathbf{F}}{\partial \boldsymbol{\Delta}} & \mathbf{I}_{np\,np\,ne} \\[2mm] \mathbf{I}_{ne\,ne\,np}^t & \mathbf{0}_{ne\,np} \end{pmatrix} \begin{pmatrix} \mathbf{D} \\[2mm] \boldsymbol{\beta} \end{pmatrix} = \begin{pmatrix} \mathbf{F} \\[2mm] \mathbf{0}_{ne} \end{pmatrix}, \qquad (25)$$

where $\mathbf{I}_{np\,np\,ne}$ is a ne-dimensional vector of np dimensional identity matrices. The components of $\partial \mathbf{F}/\partial \boldsymbol{\Delta}$ are derived in Appendix A. Ideally, $\mathbf{D}$ is equal to $\boldsymbol{\Delta}^{k+1} - \boldsymbol{\Delta}^k$. However, the step may be reduced if $\boldsymbol{\Delta}^k + \mathbf{D}$ leads to worsening the objective function (21). Therefore $\boldsymbol{\Delta}$ is updated according to

$$\boldsymbol{\Delta}^{k+1} = \boldsymbol{\Delta}^k + \alpha \, \mathbf{D}, \qquad (26)$$

where α is chosen, starting at 1, so that the updated mixing ratio matrix yields an improved objective function. Actually, a one-dimensional search is performed using the techniques described by *Gill* [1981] and *Carrera and Neuman* [1986].

[22] Only nonnegativity lateral constraints need to be imposed to solve the optimization problem, as discussed in section 2.1. To do so, when (26) yields a negative mixing ratio, δ_{pe}, its value is fixed to zero (that is, the nonnegativity constraint is activated). This constraint can be released (that

is, δ_{pe} allowed to vary), when increasing δ_{pe} may improve the objective function (i.e., when $\partial \mathscr{L}/\partial \delta_{pe} \geq 0$). Therefore at the minimum, the following conditions are satisfied:

$$\partial \mathscr{L}/\partial \delta_{pe} = 0 \qquad \text{if } \delta_{pe} > 0 \qquad (27a)$$

$$\partial \mathscr{L}/\partial \delta_{pe} \leq 0 \qquad \text{if } \delta_{pe} = 0. \qquad (27b)$$

These are termed Kuhn-Tucher conditions [*Gill*, 1981].

2.7. Implementation

[23] Actual implementation of the above method consists of the following steps. (0) Initialization ($k = 0$), which can be done by defining a set of arbitrary initial mixing ratios, $\boldsymbol{\Delta}^0$, or by least squares; the latter implies solving equation (9) and imposing nonnegativity constraints as discussed in section 2.1; (1) $k = k + 1$; (2) compute $\boldsymbol{\lambda}_s^{k+1}$ and $\boldsymbol{\mu}_s^{k+1}$ using equations (19) and (20), respectively, and substitute into (16) to obtain the objective function f^{k+1} and into (23a) to compute $\partial \mathscr{L}/\partial \boldsymbol{\Delta}$; (3) convergence test (only if $k > 0$). If $\max_{ep} |\delta_{ep}^{k+1} - \delta_{ep}^k| < \text{tolerance}$ and $|f^{k+1} - f^k| < \text{tolerance}$, then STOP. If the objective function worsens or its improvement is not sufficient, then reduce α, set $\boldsymbol{\Delta}^k = \boldsymbol{\Delta}^k + \alpha \mathbf{D}$, test constraints (that is, activate nonnegativity constraints when $\partial f/\partial \delta < 0$), and return to step 2. Otherwise, continue to step 4: (4) update $\boldsymbol{\Delta}$. Solve (25) for $\mathbf{D}$, compute $\boldsymbol{\Delta}^{k+1}$ according to (26) with $\alpha = 1$. Test non negativity constraints and go to step 1.

[24] This algorithm was programmed in FORTRAN. Preliminary tests showed that sometimes it failed to converge, in the sense that trying different initial mixing ratios $\boldsymbol{\Delta}^0$ led to different minima. When testing synthetic examples, we observed that initializing with the least squares solution is a robust option when $\mathbf{x}_s$ is not far from $\boldsymbol{\mu}_{s\,ne}$ (i.e., when end-members are relatively well known). Otherwise, uniform mixing (i.e., $\delta_{se} = 1/ne$) or random initialization may be better. Since the cost of each trial is moderate, we have opted for trying several initial mixing ratios (least squares, uniform and around 10 random perturbations) and selecting the best as solution. This approach converges in virtually every case. The resulting code is available on request or can be downloaded from http://www.h2ogeo.upc.es.

3. Application of the Methodology to Synthetic Problems

3.1. Application 1, Two End-Members

[25] This example is aimed at illustrating a case with two sources and two species. The example is inspired by Barcelona groundwater, with the two end-members being Besos River (river) and Mediterranean sea water (sea) and the two species being chloride (Cl^-) and sulphate ($SO_4^=$). Other than that, the example is totally synthetic. Basic data are presented in Tables 1 and 2. Data for the runs were obtained by randomly generating mixing ratios. These "true" ratios, together with the "true" end-member concentrations, are used to obtain the "true" concentrations of mixtures. Measurements are obtained by adding a random noise with the standard deviations of Table 2. These measurements will be used for all runs but e as shown in

Table 1. Standard Deviations for the Runs of Example 1[a]

End-Members	Species	True	Estimation Runs				
			a	b	c	d	e
River	Cl^-	200	200	200	200	200	200
River	$SO_4^=$	150	150	250	150	250	250
Sea	Cl^-, $SO_4^=$	1000	1000	1000	1000	1000	1000
All p	Cl^-	600	600	300	600	300	600
All p	$SO_4^=$	400	400	200	400	200	400
Number of samples (np)			4	4	50	50	50

[a]Concentration data for all runs have been generated using the "true" standard deviations. However, input standard deviations have been changed for each estimation run. Standard deviations are in mg/L.

Table 2. Differences between runs are restricted to the number of mixtures (4 or 50) or the input standard deviations of both end-members and mixed samples, also shown in Table 1.

[26] The first two runs are aimed at illustrating the role of the assigned standard derivations when the number of samples is small. Hence only four samples are used. In this case, the mixing line is poorly defined (Figure 4a). This reflects the noise in the measurements of mixtures. In fact, when the variance of end-members is increased and that of mixed samples is reduced without actually changing the concentrations (run b), the effect of noise in the latter is emphasized. As a result, concentration of species ($SO_4^=$) in end-member (river) becomes negative (Figure 4b and Table 2).

[27] It might be argued that concentrations should be constrained to be positive (the same as proportions). We have found, however, that negative concentrations are a very rare event, practically restricted to end-members and to situations where inappropriate parameters were specified such as artificially increasing the variance of the end-members while reducing the variance of the mixtures, and when the number of samples was small. When the variances are fixed (run a) or the number of samples increased to 50 (run d), or both (run c), the problem is fixed (Table 2 and Figure 4).

[28] Further examination of Table 2 makes it apparent that the concentration of Cl^- is consistently underestimated. This reflects the very small measured value of Cl^- in some mixed samples. Sometimes, it reflects the opposite (namely, that end-member measurements are far away from the interval of mixture measurements, recall Figure 3). In both cases, the problem is fixed by perturbing measurements of end-member concentrations toward the center of gravity of all concentration measurements while keeping a relatively

large variance. This is what motivates run e (Table 2), which indeed leads to improved estimates of end-members. In practical situations, however, it may not be easy to assess the validity of such concentrations.

3.2. Application 2, Three End-Members

[29] This example is aimed at illustrating the benefits of redundancy (large number of samples and species) upon the estimation of both end-members concentrations and mixing ratios. The formulation of the test is analogous to that of previous section.

[30] 1. Start with perfectly known concentrations of five hypothetical species at three end-member waters. These are shown in Table 3.

[31] 2. Generate 100 mixed samples from 100 uniformly distributed mixing ratios sets. These will be termed "true" mixing ratios.

[32] 3. Measured data are generated by adding a random noise with varying standard deviation (see Table 3) to both end-members and mixed samples. Notice that the standard deviation is much larger for end-members waters than for mixed samples. Two sets of end-members have been generated (low and high variance). All these data are shown in Figure 5.

[33] 4. Results are evaluated in terms of several indices: mixing ratios average absolute error; correlation between true and computed mixing ratios; improvement index for end-member concentrations, defined as

$$IM = ns \, ne \left[\sum_{s=1}^{ns} \sum_{e=1}^{ne} \frac{(x_{se} - \mu_{se})^2}{\sigma_{se}^2} \right]^{-1}. \quad (28)$$

This latter index measures the improvement caused by estimation (IM = 2 implies that the mean square error of end-member concentrations has been reduced by a factor of two during estimation).

[34] Figure 6a displays the evolution of correlation coefficients between true and estimated mixing ratios for varying number of samples. A number of issues deserve discussion. First, in general, correlation grows with the number of samples. This observation is consistent with the motivation of our work. That is, data from one sample help estimating the others. Obviously, this contrasts with least squares, where mixing ratios are estimated independently for each sample, so that they do not benefit from each other. Still, results are comparable for a small number of samples (actually, least squares slightly outperforms likelihood in the low noise case with only four samples). Second, the proposed method yields results that are significantly

Table 2. Concentrations of End-Members[a]

End-Members	Species	True	Measured (Input)[b]	Computed for Each Run				
				a	b	c	d	e
River	Cl^-	478	143 (600)	157	179	117	130	511
River	$SO_4^=$	244	102 (400)	49	−237	210	264	337
Sea	Cl^-	21,050	19,405	19,504	19,503	19,971	20,097	19,985
Sea	$SO_4^=$	2910	3611	2946	3022	2837	2621	2804
Number of samples (np)				4	4	50	50	50

[a]Input values, representing measurements, were generated from the true values using noise with the standard deviations of Table 1. Concentrations are in mg/L.

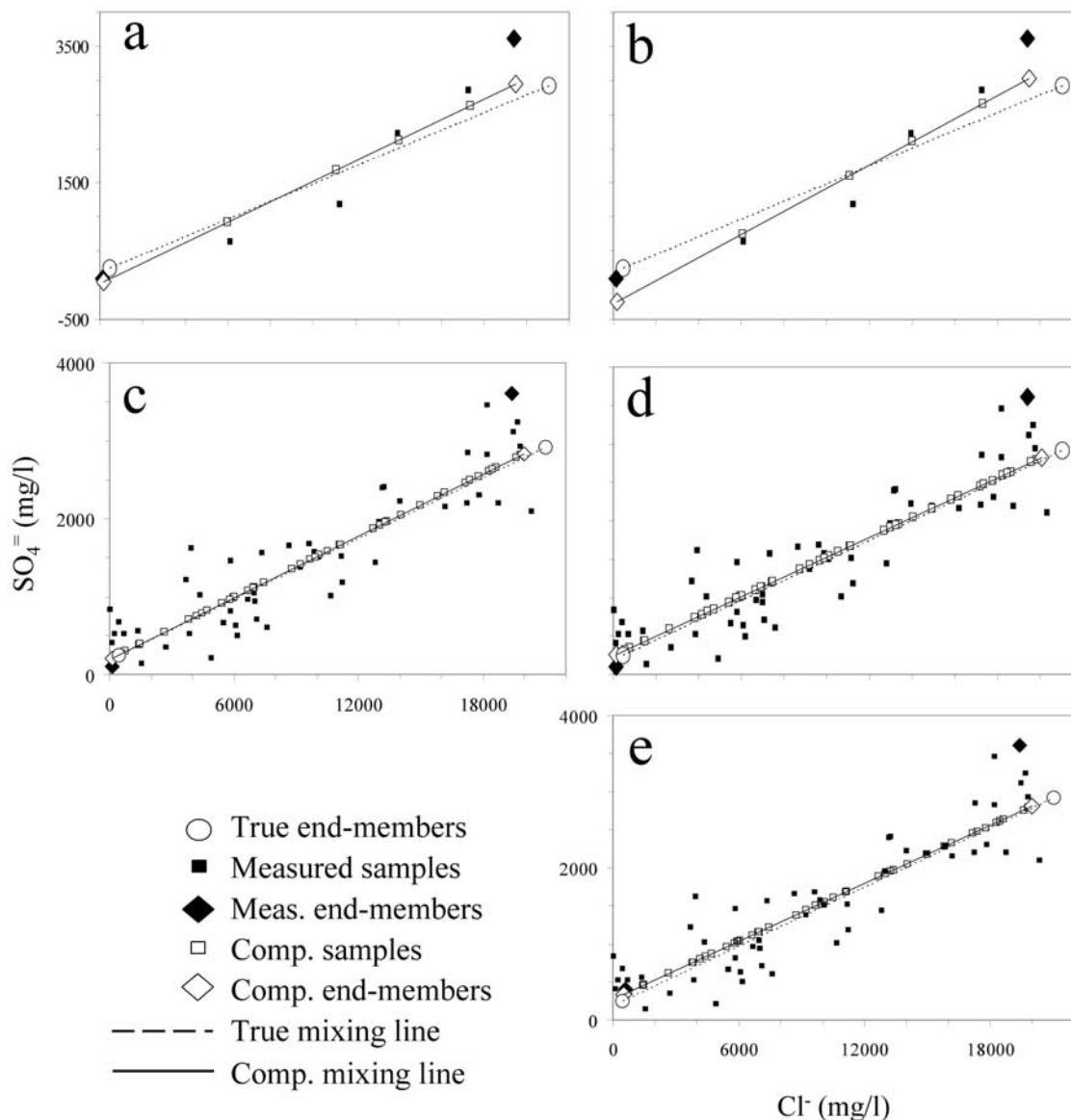[b]Measured values of end-member concentrations for all runs but e (values in parentheses).

Figure 4. Results of example 1. Only four samples are used in runs a and b. This leads to poor mixing lines and estimation of end-member concentrations. Moreover, results are quite sensitive to small variations in input standard derivations, leading to negative concentrations in end-member 1 (run b). Mixing lines are much better and less sensitive to input statistics when 50 samples are used (runs c and d). In this example, computed end-member concentrations are slightly improved if input ''measurements'' are well within the interval of mixed samples measurements (run e).

better than least squares except for the four samples case. Correlations for the likelihood method are consistently above 0.99 when more than 10 samples are used, and reach up to 0.998 for 100 samples. Least squares estimates, on the other hand, fluctuate between 0.97 and 0.98, when using small error end-member concentrations, or between 0.93 and 0.94 in the large error case. Finally, when the number of samples is moderate (more than 10), correlations exhibit negligible sensitivity to the size of errors in end-member concentrations. Again, this contrasts with least squares estimates, whose quality degrades significantly with increasing errors.

[35] Similar results can be observed in terms of the average absolute error of estimated mixing ratios (Figure 6b). The main difference is that, now, least squares outperforms

likelihood in the four samples case, both for small and large errors in input end-member concentrations. Obviously, this reflects a random fluctuation because the average error of least squares estimates, which is independent of the number of wells, is larger than that of the likelihood method. However, this observation stresses that the real benefit of the proposed method comes from increasing the number of wells, which causes errors in mixing ratios to drop to nearly 0.01, with little sensitivity to errors in end-member concentrations.

[36] Finally, the improvement index is shown in Figure 6c. It is clear that estimated end-member concentrations are much better than their input counterparts. The improvement index grows from 3, in the case of four samples, to 8 for 100 samples. In fact, it is this improvement

Table 3. True End-Member Concentrations and Standard Deviations of Noise in Example 2[a]

	Species				
	1	2	3	4	5
True Concentrations					
End-member 1	500	700	100	800	200
End-member 2	100	100	400	200	700
End-member 3	700	400	900	500	50
Standard Deviations (Low-Variance Noise)					
End-member 1	100	100	50	100	50
End-member 2	50	50	100	50	100
End-member 3	100	100	100	100	25
Standard Deviations (High-Variance Noise)					
End-member 1	200	200	75	200	75
End-member 2	75	75	200	75	200
End-member 3	200	200	200	200	30

[a]Mixed samples standard deviation = 4.

what caused the reduction in mixing ratios errors with increasing number of samples shown in Figures 6a and 6b.

4. Summary and Discussion

[37] The problem addressed in this paper consists of estimating mixing ratios from the concentrations of different conservative species in a water sample. Solute concentrations at any water sample come from the weighted average of end-members concentrations, where the weights are the mixing ratios. One of the main problems of traditional techniques for computing mixing ratios is the uncertainty in end-member concentration of each solute. This uncertainty may stem from conceptual errors and from both spatial and temporal variability, so that pure end-members may not exist. As a result it is generally not easy to establish the representativity of an end-member sample. On the other hand, errors in mixtures concentrations should be much smaller than those of end-members. Because of this, mixtures may contain much information about end-members, which is what motivates our work.

[38] We have presented here a method that uses concentrations of mixtures to condition mixing calculations, while acknowledging that concentrations of end-members are uncertain. The method should be especially useful when many mixtures are available. In fact, joint use of all data is the basis for the improvements of our method over traditional approaches. In these, uncertainty is only accounted for a posteriori and mixing proportions are estimated for individual samples assuming perfectly known end-members [e.g., *Williams et al.*, 2001; *Yang et al.*, 1999]. At best it is possible to do a statistical analysis of the mixing proportions [*Pitkänen et al.*, 1999; *Plummer et al.*, 1998; *Skov et al.*, 1997], or use a priori a Monte Carlo approach to account for time variability in the end-members [*Joerin et al.*, 2002]. These approaches work best when end-members are indeed constant in space and time and display low uncertainty [*Allègre et al.*, 1996]. However, when end-members are variable the proposed method should be used. Acknowledging the uncertainty in end-members leads to an improvement not only on the estimation of actual end-member concentrations but, more importantly, on the computation of mixing ratios.

[39] For a given mixing problem, our methodology requires specifying measured concentrations of both mixed samples and end-members plus measurement errors (in practice, standard deviations). In this sense it needs the same amount of information as other methods based on least squares [e.g., *Allègre and Lewin*, 1989]. There is always some uncertainty about the size of measurement errors. Laboratories often specify an evaluation of the magnitude of analytical errors (confidence intervals). This, possibly enlarged to account for sample contamination during handling, should be sufficient for evaluating uncertainty of mixture concentrations. However, errors in end-members involve conceptual decisions that must be addressed individually in each case. For example, river recharge may be restricted to sporadic flood events, when concentrations are very different from the mean. In such case, a continuous record of concentrations would be of little use if one does not know when inflow takes place. That is, standard deviations may be difficult to assign and a sensitivity analysis should be performed in each case. Yet, the synthetic applications discussed here suggest that the proposed method is robust with respect to moderate errors in the assumed standard deviations.

[40] The example case of flooding rivers points to a more challenging difficulty. Mixing calculations assume implicitly that the concentrations of inflows are the same for all mixtures. This may be true when inflow concentrations fluctuate with a high frequency (mixing tends to dampen out these fluctuations). However, it may not be appropriate for slow fluctuations. In this case, however, the problem lies in the model concept: simple mixing calculations are not appropriate and one may need to perform more complex transport calculations. Even here, ingenuous use of the method may shed some light on the underlying processes. For example, differences between computed and measured end-member concentrations may suggest changes in the conceptual model. Also, using two end-members to represent river water (water quality of high and low flows) may help in separating these two components of inflow. That is, when done properly, the scope of mixing calculations can be significantly expanded.

[41] Mixing calculations are often viewed in hydrology as a preliminary step in the process of building a conceptual model of where water comes from. These calculations are frequently followed by more complex models. Although this approach need not change, we wish to stress two main points in our research findings. First, these calculations can be misleading when end-members are uncertain. Second, they can be greatly improved upon with little additional cost whenever many mixed samples are available. In fact, by yielding end-members concentrations possibly different from measurements, our method may point to inconsistencies in the original conceptual model and suggest how to modify it.

Appendix A: Computation of $\partial F/\partial \Delta$

[42] Using equation (23a) for $\mathbf{F}$ and taking derivatives leads to

$$\frac{\partial F_{ij}}{\partial \delta_{kl}} = \sum_{s=1}^{ns} \left(\frac{\partial \lambda_{si}}{\partial \delta_{kl}} \mu_{sj} + \lambda_{si} \frac{\partial \mu_{sj}}{\partial \delta_{kl}} \right) \begin{matrix} i, k = 1, \cdots, np \\ j, l = 1, \cdots, ne \end{matrix}. \quad (A1)$$
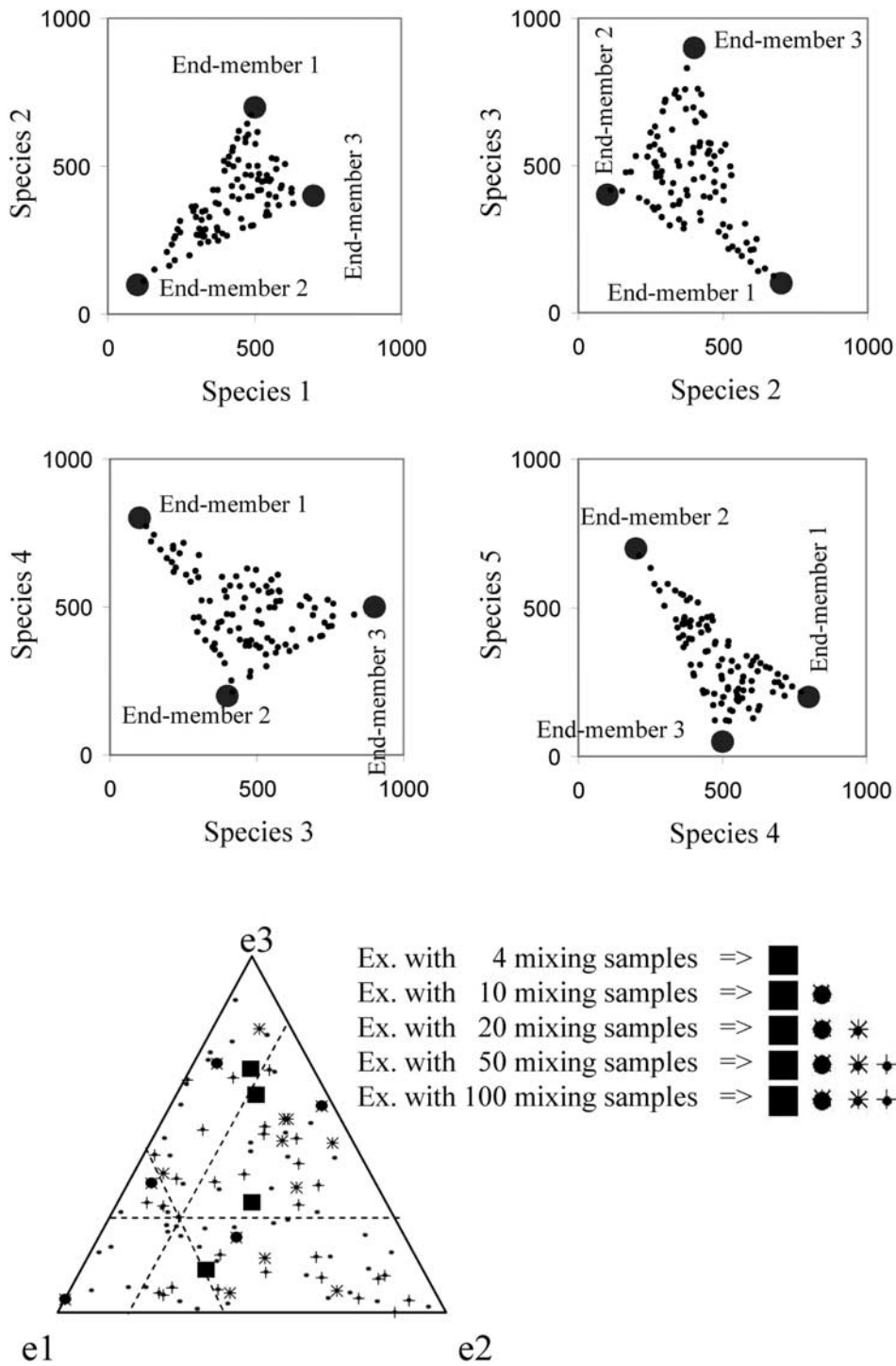
Figure 5. Data for example 2. (top) Concentrations of all species in end-members and mixed waters. (bottom) Mixing ratios. The symbol identifies the mixed waters used in each run. Data used in the run with four samples were also used in the runs with 10, 20, 50, and 100 samples. Similarly, data used in the run with 10 samples were also used in the runs with 20, 50, and 100 samples, etc.

We now substitute (19) into (A1) to simplify the first term of the right hand side. We use the fact that

$$\frac{\partial \boldsymbol{\lambda}_s}{\partial \boldsymbol{\Delta}} = \mathbf{C}_s \frac{\partial \boldsymbol{\Gamma}}{\partial \boldsymbol{\Delta}} \mathbf{b}_s, \qquad (A2)$$

where $\mathbf{b}_s = 2\widehat{\boldsymbol{\varepsilon}}_s - \mathbf{z}_s$, and $\widehat{\boldsymbol{\varepsilon}}_s = \mathbf{z}_s - \boldsymbol{\mu}_s$ is the estimate of measurement errors. As $\partial \Gamma_{uv}/\partial \delta_{kl} = 1$, if $n = k$ and $v = l$, the first summand in the right hand side of (A1) becomes

$$\frac{\partial \lambda_{si}}{\partial \delta_{kl}} \mu_{sj} = C_{sik} \, b_{sl} \mu_{sj}. \qquad (A3)$$
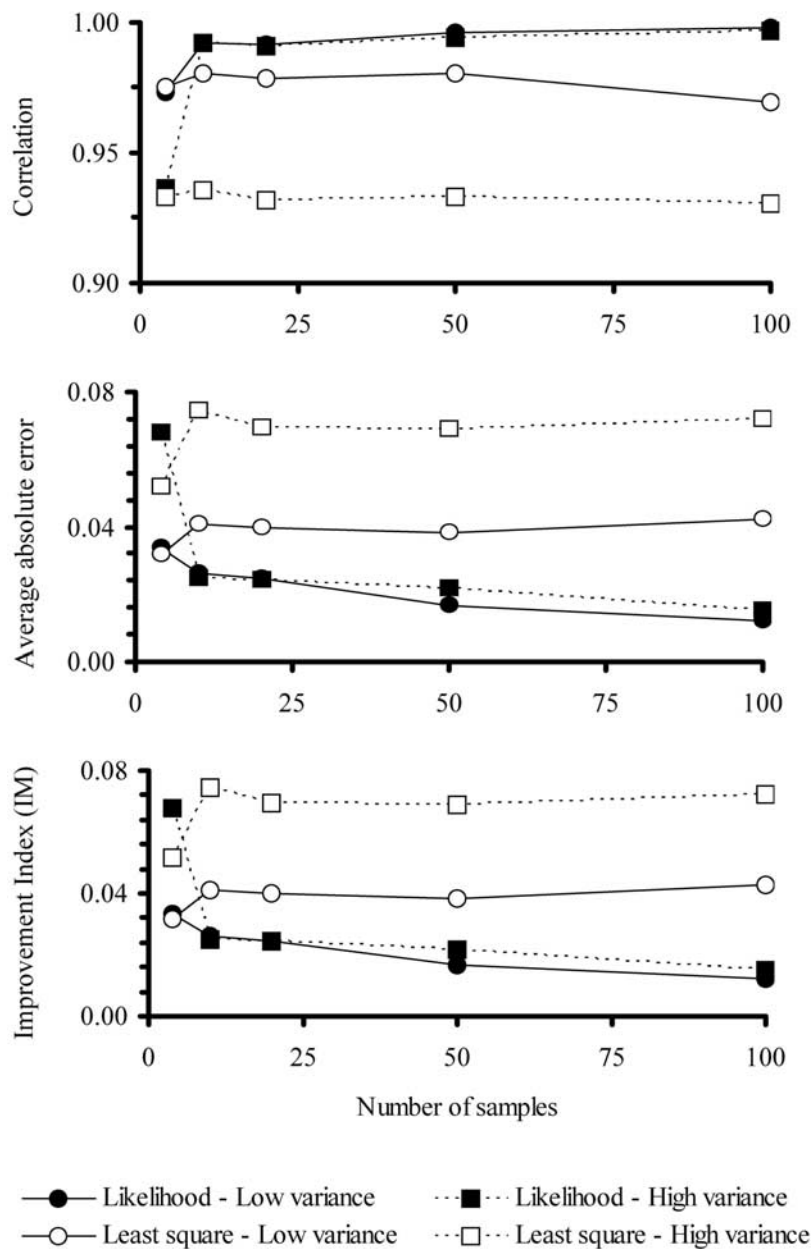
Figure 6. Results of example 2 as a function of the number of samples. (top) Correlation between computed and true mixing ratios improves with increasing number of samples in the likelihood method, thus yielding much better results than conventional least squares, which does not depend on the number of samples. Notice also that contrary to least squares, likelihood results display little sensitivity to the noise of end-member concentration measurements. (middle) Average absolute error in estimated mixing ratios is reduced as the number of samples is increased, in contrast to least squares, which displays no improvement. (bottom) Improvement index (equation (28)) also shows that the estimated end-member concentrations improve with the number of samples.

Similarly, the second summand is developed by first noting that we are just seeking the first ne components of μ_s (20). These are given by

$$\mu_{sne} = \mathbf{x}_s - \mathbf{A}_{sne}\mathbf{\Gamma}^t\mathbf{C}_s\mathbf{\Gamma}z_s, \tag{A4}$$

where $\mathbf{A}_{sne}$ represents the top ne rows of $\mathbf{A}_s$ (i.e., those involving the covariances of end-member concentrations of species s among themselves and with those of sampling points). Taking derivatives of this expression yields

$$\frac{\partial \mu_{sne}^t}{\partial \mathbf{\Delta}} = \left(-\mathbf{z}_s^t \frac{\partial \mathbf{\Gamma}^t}{\partial \mathbf{\Delta}} \mathbf{C}_s\mathbf{\Gamma} - 2\lambda_s^t \frac{\partial \mathbf{\Gamma}}{\partial \mathbf{\Delta}} \mathbf{A}_s\mathbf{\Gamma} + \lambda_s^t \frac{\partial \mathbf{\Gamma}}{\partial \mathbf{\Delta}} \right) \mathbf{A}_{sne}. \tag{A5}$$

Here, we have made use of the expression of $\mathbf{C}_s$ and the rules for deriving the inverse of a matrix. We now define

$$\mathbf{P} = \mathbf{C}_s\mathbf{\Gamma}\mathbf{A}_{sne} \qquad \mathbf{U} = \mathbf{A}_s\mathbf{\Gamma}^t\mathbf{P}. \tag{A6}$$

Using these definitions and (A5), the second term in the right hand side of (A1) can be expressed components-wise as

$$\lambda_{si}\frac{\partial \mu_{sj}}{\partial \delta_{kl}} = x_{si}\left(-z_{sl}P_{kj} - 2\lambda_{sk}U_{lj} + \lambda_{sk}\mathbf{A}_{slj} \right). \tag{A7}$$

Adding this to (A3) and summing up over all species yields $\partial F_{ij}/\partial \delta_{kl}$, which is what we were seeking.

References

Adar, E. M., and R. Nativ (2000), Use of hydrochemistry and isotopes in a mixing-cell to quantify the relative contribution of multiple-source contaminants to seepage from fractured chalk aquitard, *IAHS Publ.*, *262*, 315–320.

Adar, E. M., S. P. Neuman, and D. A. Woolhiser (1988), Estimation of spatial recharge distribution using environmental isotopes and hydrochemical data. I. Mathematical model and application to synthetic data, *J. Hydrol.*, *97*, 251–277.

Adar, E. M., E. Rosenthal, A. S. Issar, and O. Batelaan (1992), Quantitative assessment of flow pattern in the southern Arava Valley (Israel) by environmental tracer in a mixing cell model, *J. Hydrol.*, *136*, 333–352.

Allègre, C. J., and E. Lewin (1989), Chemical structure and history of the Earth: Evidence from global non-linear inversion of isotopic data in a three-box model, *Earth Planet. Sci. Lett.*, *96*, 61–88.

Allègre, C. J., B. Dupre, P. Négrel, and J. Gaillardet (1996), Sr-Nd-Pb isotope systematics in Amazon and Congo River systems: Constraints about erosion processes, *Chem. Geol.*, *131*, 93–112.

Biesenthal, T. A., and P. B. Shepson (1997), Observations of anthropogenic inputs of the isoprene oxidation products methyl vinyl ketone and methacrolein to the atmosphere, *Geophys. Res. Lett.*, *24*, 1375–1378.

Campana, M. F., and E. S. Simpson (1984), Groundwater residence times and discharge rates using discrete state compartment model and 14C data, *J. Hydrol.*, *72*, 171–185.

Carrera, J., and S. P. Neuman (1986), Estimation of aquifer parameters under steady-state and transient conditions: 1. Background and statistical framework, *Water Resour. Res.*, *22*, 199–210.

Castillo, O. (2000), Mètode general per a la quantificació de la recàrrega en una àrea urbana: Aplicació al cas de Barcelona (General method for quantifying urban groundwater recharge: The Barcelona city case), B.S. thesis, 92 pp., Tech. Univ. of Catalonia, Barcelona, Spain.

Custodio, E., and M. R. Llamas (1984), *Hidrología Subterránea*, 2350 pp., Omega, Barcelona, Spain.

Gill, R. D. (1981), Testing with replacement and the product limit estimator, *Ann. Stat.*, *9*, 853–860.

Joerin, C., K. J. Beven, I. Iorgulescu, and A. Musy (2002), Uncertainty in hydrograph separations based on geochemical mixing models, *J. Hydrol.*, *255*, 90–106.

Johnson, C. A., M. A. Mast, and C. L. Kester (2001), Use of $^{17}O^{16}O$ to trace atmospherically-deposited sulfate in surface waters: A case study in alpine watersheds in the Rocky Mountains, *Geophys. Res. Lett.*, *28*, 4483–4486.

Kent, J. T., G. S. Watson, and T. C. Onstott (1990), Fitting straight lines and planes with an application to radiometric dating, *Earth Planet. Sci. Lett.*, *97*, 1–17.

Medina, A., and J. Carrera (1995), Joint inversion of head and concentration data application to regionalized transmissivity (abstract), *Ann. Geophys.*, *12*, C-478.

Ojiambo, B. S., R. J. Poreda, and W. B. Lyons (2001), Groundwater/surface water interaction in Lake Naivasha, Kenya, using delta 0-18, delta D and He-3/He-3 age dating, *Ground Water*, *39*, 526–533.

Pitkänen, P., J. Löffman, L. Koskinen, H. Leino-Forsman, and M. Snellman (1999), Application of mass-balance and flow simulation calculations to interpretation of mixing at Äspö, Sweden, *Appl. Geochem.*, *14*, 893–905.

Plummer, L. N., E. Busenberg, and S. Drenkard (1998), Flow of river water into a karstic limestone aquifer. 2. Dating the young fraction in groundwater mixtures in the Upper Floridian aquifer near Valdosta, Georgia, *Appl. Geochem.*, *13*, 1017–1043.

Roy, S., J. Gaillardet, and C. J. Allègre (1999), Geochemistry of dissolved and suspended loads of the Seine River, France: Anthropogenic impact, carbonate and silicate weathering, *Geochim. Cosmochim. Acta*, *63*, 1277–1292.

Skov, H., A. H. Egelov, K. Granby, and T. Nielsen (1997), Relationships between ozone and other photochemical products at Ll, Valby, Denmark, *Atmos. Environ.*, *31*, 685–691.

Stute, M., J. Deak, K. Revesz, J. K. Bohlke, E. Deseo, R. Wappernig, and P. Schlosser (1997), Tritium/He-3 dating of river infiltration: An example from the Danube in the Szigetkoz area, Hungary, *Ground Water*, *35*, 905–911.

Suk, H., and K.-K. Lee (1999), Characterization of ground water hydrochemical system through multivariate analysis: Clustering into ground water zones, *Ground Water*, *37*, 358–366.

Vázquez-Suñé, E., X. Sánchez-Vila, J. Carrera, M. Marizza, R. Arandes, and L. A. Gutierrez (1997), Rising of groundwater level in Barcelona: Evolution and effects on urban structures, in *Groundwater in the Urban Environment*, edited by J. Chilton et al., pp. 267–271, A. A. Balkema, Brookfield, Vt.

Williams, M. R., A. Leydecker, A. D. Brown, and J. M. Melack (2001), Processes regulating the solute concentrations of snowmelt runoff in two subalpine catchments of the Sierra Nevada, California, *Water Resour. Res.*, *37*, 1993–2008.

Yang, Y., D. N. Lerner, M. Barret, and J. Tellam (1999), Quantification of groundwater recharge in the city of Nottingham, UK, *Environ. Geol.*, *38*, 183–198.

Zuber, A. (1986), Mathematical models for the interpretation of environmental radioisotopes in groundwater systems, in *Handbook of Environmental Isotope Geochemistry*, vol. 2, edited by P. Fritz and J. C. Fontes, pp. 1–59, Elsevier, New York.

————————————————

J. Carrera, O. Castillo, X. Sánchez-Vila, and E. Vázquez-Suñé, Department Geotechnical Engineering and Geosciences, School of Civil Engineering, Technical University of Catalonia, Barcelona, Catalonia 08034, Spain. (jesus.carrera@upc.es; olga.castillo@upc.es; xavier.sanchez-vila@upc.es; enric.vazquez-sune.upc.es)